Severe and progressive encephalitis as a presenting manifestation of a novel missense perforin mutation and impaired cytolytic activity

Jérôme Feldmann, Gaël Ménasché, Isabelle Callebaut, Véronique Minard-Colin, Brigitte Bader-Meunier, Laurence Le Clainche, Alain Fischer, Françoise Le Deist, Marc Tardieu, and Geneviève de Saint Basile

Mutations in the perforin gene cause familial hemophagocytic lymphohistiocytosis (FHL). The first symptoms of FHL are usually intractable fever, hepatosplenomegaly, and pancytopenia. Most FHL patients subsequently develop central nervous system (CNS) manifestations due to infiltration of tissues by activated lymphocytes and macrophages. We report 2 FHL patients with an atypical phenotype characterized by isolated severe neurologic symptoms mimicking chronic encephalitis and leading to an early death. Functional and molecular analyses revealed the same novel missense mutation in the perforin gene in both patients; this mutation affected the calcium-binding domain of the protein. This missense mutation did not affect perforin maturation or expression in cytotoxic cells but impaired in vitro cytotoxic activity. Diagnosis was delayed in both patients because of the initial neurologic expression and the normal expression of perforin in circulating lymphocytes. This emphasizes the importance of early diagnosis of this atypical form of FHL, as CNS involvement causes severe, irreversible encephalopathy. This observation also raises the question of the role of some mutations in the neurologic expression of FHL. (Blood. 2005; 105:2658-2663)

Introduction

Familial hemophagocytic lymphohistiocytosis (FHL) is an autosomal recessive disorder caused by several different mutations. For example, FHL2 is caused by a mutation in the gene coding for the T-lymphocyte cytotoxic effector perforin,[1] and FHL3 results from a mutation in the gene encoding mammalian homolog of *Caenorhabditis elegans* uncoordinated 13 mutant phenotype (Munc13)–4, a recently identified effector of the cytotoxic pathway.[2] The disease is characterized by the persistent proliferation and activation of T lymphocytes, mainly $CD8^+$, and macrophages that infiltrate organs such as bone marrow, lymph nodes, spleen, and liver, leading to severe tissue necrosis.[3] Neurologic symptoms commonly develop during the course of this syndrome.[4,5] However, in a few patients, isolated neurologic symptoms mimicking persistent encephalitis precede nonneurologic symptoms by several months or remain isolated until death.[6,7] Correct diagnosis is of utmost importance in these patients, as early bone marrow transplantation can prevent further deterioration and as the disease might affect offspring. Diagnosis is usually based on the detection of hemophagocytosis in bone marrow aspirate associated with pancytopenia, coagulation abnormalities, hepatitis, hypertriglyceridemia, and hyperferritinemia.[8] Similarly, study of surface antigens on lymphocytes can demonstrate T-cell activation (including increased expression of major histocompatibility complex [MHC] class II surface antigens).[9] Granule-dependent cytotoxicity analysis, expression of perforin in lymphocytes and natural killer (NK) cells, and the detection of gene mutations can lead to a precise molecular diagnosis.[1,2]

In this report, we describe 2 FHL patients presenting an acute, encephalitis-like, neurologic disease. Functional and genetic analyses showed that the disease was caused by the same missense mutation in the perforin gene in both patients. This mutation did not affect perforin expression in cytotoxic cells but impaired perforin function, potentially through its ability to bind calcium.

Patients, materials, and methods

Genotype analysis and mutation detection

Blood samples were obtained from patients, relatives, and controls. Approval was obtained from l'Institut National de la Santé et de la Recherche Médicale (INSERM) Institutional Review Board for these studies. Informed consent was provided according to the Declaration of Helsinki. DNA was extracted from peripheral blood mononuclear cells (PBMCs) by using standard methods. Polymorphic microsatellite markers mapping to the perforin locus on chromosome 10q21 (D10S1688, D10S537, D10S1650) were analyzed for homozygosity in the 2 consanguineous families, as previously described.[1,10] The primers for the amplification of the 2 coding exons of perforin (exons 2 and 3) as well as the polymerase chain reaction (PCR) conditions have been previously described.[1] PCR

From the Institut National de la Santé et de la Recherche Médicale (INSERM) U429, Hôpital Necker-Enfants Malades, Paris, France; Laboratoire de Minéralogie-Cristallographie Paris (LMCP), Centre National de la Recherche Scientifique (CNRS) UMR7590, Universités Paris 6 and Paris 7, Paris, France; Unité d'Immunologie-Hématologie, Hôpital Necker-Enfants Malades, Paris, France; Département de Pédiatrie, et Service de Neurologie, Hôpital Bicêtre, Le Kremlin-Bicêtre, France; and Service de Pédiatrie, Centre Hospitalier René Dubos, Cergy Pontoise, France.

Submitted September 15, 2004; accepted November 9, 2004. Prepublished online as *Blood* First Edition Paper, December 14, 2004; DOI 10.1182/blood-2004-09-3590.

Supported by grants from INSERM, l'Association de Recherche sur le Cancer (ARC), and l'Association Vaincre les Maladies Lysosomales (VML).

An Inside *Blood* analysis of this article appears in the front of this issue.

Reprints: Geneviève de Saint Basile, INSERM U429, Hôpital Necker-Enfants Malades, 149 rue de Sèvres, 75743 Paris, Cedex 15, France; e-mail: sbasile@necker.fr.

The publication costs of this article were defrayed in part by page charge payment. Therefore, and solely to indicate this fact, this article is hereby marked "advertisement" in accordance with 18 U.S.C. section 1734.

products were directly sequenced in both directions using the Dye Terminator Cycle Sequencing Ready Reaction Kit (Perkin Elmer, Shelton, CT).

C2 domain alignment and modeling

Superimposition of the known 3-dimensional structures of C2 domains allowed their structural alignment, which was then used to align the C2 domain of perforin. Hydrophobic cluster analysis[11] was used to refine the alignment in difficult regions, such as the sequence including strands β7 and β8, for which our proposition slightly differs from that of Uellner et al.[12]

Three-dimensional structures were manipulated using Swiss-PDB-viewer (Swiss Institute of Bioinformatics, Basel, Switzerland).[13] Modeller-4 (University of California at San Francisco),[14] running at the bioserv server (http://bioserv.cbs.cnrs.fr/), was used for 3-dimensional modeling.

Immunologic investigations

Immunofluorescence. The following monoclonal antibodies (MoAbs) were used: anti-CD3: Leu 4 (immunoglobulin G2a [IgG2a]; Becton Dickinson [BD], San Diego, CA); anti-CD8: Leu 2a (IgG1, BD); anti–T-cell receptor αβ (anti-TCRαβ): BMA031 (IgG1; Immunotech, Marseille, France); anti-CD4: Leu 3a (IgG1, BD); anti-CD56 (IgG1, Immunotech); anti–HLA DR: L243 (IgG2a, BD). Except when otherwise indicated, phycoerythrin (PE)–, fluorescein isothiocyanate (FITC)–, or PE-Cy5 (PC5)-conjugated MoAbs were used for fluorescence staining of whole blood samples.

Perforin expression in cytotoxic cells was evaluated by flow cytometry. Whole blood collected on EDTA (ethylenediaminetetraacetic acid; 100 μL) was first incubated for 30 minutes at 4°C in phosphate-buffered saline (PBS) with labeled antibodies to detect membrane antigens. The red blood cells were lysed by Facs-lysing solution (BD), then fixed and permeabilized by Facs-permeabilizing solution (BD) according to the manufacturer's recommendations. Cells were washed twice in PBS with 0.5 mg/mL of bovine serum albumin (BSA; Sigma, Saint Quentin Fallavier, France) and 0.02% sodium azide (Sigma) and incubated for 30 minutes at 4°C with FITC-conjugated antiperforin (IgG2b; Ancell, Bayport, MN). The cells were then analyzed on a FACScalibur flow cytometer (BD). We recorded 2×10^4 events gating on PBMCs and excluded dead cells, monocytes, and polynuclear cells based on forward scatter/side scatter (FSC/SSC) criteria.

Functional analyses. Cytotoxic activity was measured as previously described.[1] Briefly, PBMCs from patients, parents, or healthy controls were cultured with PHA (phytohemagglutinin; 1:700 dilution; Difco, Detroit, MI) and interleukin 2 (IL-2; 20 IU/mL; Valbiotech, Compiegne, France) for 24 hours. The IL-2 concentration was then increased (40 IU/mL) for 6 days. For the cytotoxic activity assay, lysis of Fas-deficient L1210-3 target cells (10^4 L1210 cells loaded with chromium^{51}) was measured in a standard 4-hour release assay in the presence of a monoclonal anti-CD3 antibody (10 μg/mL; OKT3; Ortoclone, Jansen, France). The effector-target ratio was calculated from the number of $CD8^+$ T cells as determined by flow cytometry.

The degranulation assay was performed as previously described with some modifications.[15] Briefly, 96-well plates that had been coated with anti-CD3 antibody (20 μg/mL; OKT3; Ortoclone) were used instead of target cells to stimulate 6×10^5 T cells/well in a 4-hour release assay. The release of BLT (N-a-benzyloxycarbonyl-L-lysine thiobenzyl ester) esterase was measured as previously described with a 50-μL aliquot of cell-free supernatant.[15]

Results

Case report

Patient 1 was the third child of consanguineous parents from Algeria. There was no known family history of neurologic disease or early death. Three other siblings were healthy. The patient was hypotrophic at birth (weight 2300 g, length 47 cm, and head circumference 30 cm at 39 weeks gestation). Neurologic symptoms were first noted at 5 months of age after an acute and apparently benign upper respiratory infection: poor head control, tremor of extremities, and abnormal postural tone for age. The patient was hospitalized 2 months later because of the onset of seizures, status epilepticus, ataxia, and coma without fever. Within 2 weeks, the patient developed persistent myoclonus, pyramidal rigidity of lower limbs, right facial weakness, and impaired ocular movements. Two brain magnetic resonance imagings (MRIs) were performed 3 weeks apart at the age of 8 months. Large areas of white matter at periventricular, deep supratentorial, and cerebellar locations were hyperintense in relaxation time (T) 2-weighted and fluid-attenuated inversion recovery (FLAIR) images and hypointense on T1-weighted images and showed contrast enhancement after application of gadolinium (Figure 1A-B). There was also evidence of lesions in the corpus callosum and brain stem mostly in the tegmentum and the pons. No subcortical, cortical, or basal ganglia abnormalities were detected. Lesions were larger on the second MRI. In addition, a moderate degree of hepatosplenomegaly and a 5-cm right cervical mass were detected.

Results of laboratory investigations are shown in Table 1. The absolute lymphocyte count was normal at that time, while slightly decreased 2 months later with normal percentages of CD4, CD8, and B and NK lymphocytes. No excess of activated DR^+ T cells was found. The serum immunoglobulin level and the antibody responses were normal (not shown). Clonal proliferation of T or B lymphocytes was not detected in bone marrow or cerebral spinal fluid (CSF). Chronic lymphocytic meningitis associated with anemia, thrombocytopenia, and hypoferritinemia was detectable at the age of 7 months, while hyponatremia and a slightly elevated triglyceride concentration were detected 2 months latter. Liver enzyme levels remained normal. There was no evidence of hemophagocytosis in CSF cells or bone marrow aspirate. CSF lactate level was elevated. The serum lactate–pyruvate (L/P) ratio was lower (maximum lactate concentration, 2.5 mM; L/P ratio, 22), suggesting a metabolic disorder. Serum, urine amino acid, and urine organic acid analyses were normal, as was a direct investigation of lymphocytic respiratory chain complex activities. Lead concentration was in the normal range.

No underlying infection was found despite extensive examinations, including mycobacteria, herpes simplex virus (HSVA-C), Epstein-Barr virus (EBV), cytomegalovirus (CMV), human immunodeficiency virus (HIV), *Mycoplasma pneumoniae,* Lyme disease, leptospirosis, *Rochalimaea henselae*, bacteria, and fungi. Histologic examination of the enlarged lymph node showed necrosis and inflammatory cells. Histologic analysis of the liver biopsy showed lymphoid infiltrates with mostly $CD3^+$ T cells and signs of macrophage activation.

The patient's condition steadily worsened with persistent seizures despite antiepileptic treatment and coma leading to death at

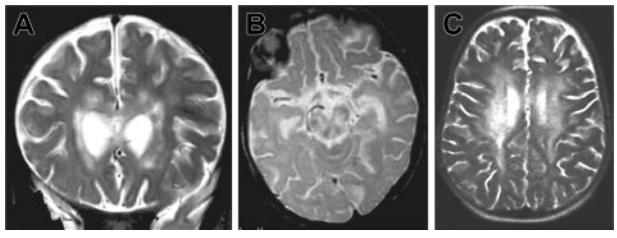

Figure 1. Brain magnetic resonance images of patients 1 and 2. MRIs show large white matter lesions in periventricular areas and brain stem. (A) Patient 1, 7 months, coronal T2 section. (B) Patient 1, 7 months, sagittal T2 section. (C) Patient 2, 33 months, sagittal T2 section.

Table 1. Laboratory investigations

	Patient 1		Patient 2		
	7 mo*	9 mo*	30 mo*	33 mo*	Normal values
Hemoglobin level, g/dL	8.2	11	11.7	6.2	11-13
Neutrophil count, 10^9/L	2.6	5.0	2.35	0.85	> 1.5
Platelet count, 10^9/L	117	130	148	17	150-400
Fibrinogen level, g/L	2.1	3	NE	2.9	2-4
Ferritin level, μg/L	10	72	NE	166	14-197
Triglyceridemia level, mM	1.1	2.6	NE	3.3	0.4-1.2
Serum sodium level, mM	138	127	135	127	136-146
Transaminase level; ALT-AST, IU/L	22	38	14/40	12/38	7-60
Lactate level, mM	NE	2.5	NE	1.17	0.5-1.95
CSF investigation					
Cell count, 10^6/L	25	75	NE	30	< 10
Protein level, g/L	1.1	2.6	NE	1.19	< 0.3
Glucose level, mM	0.9	1.5	NE	2.49	2.5-4
Lactate level, mM	NE	3.5	NE	3.62	1.1-2.2
Immunologic investigation					
Lymphocyte count, 10^9/L	8.170	1.640	NR	NR	4.000-13.500†
Lymphocyte subset, %	NR	NR	15.792	0.900	4.000-9.000‡
CD3	NE	59	NE	67	60-80
CD4	NE	40	NE	53	35-50
CD8	NE	15	NE	12	15-35
HLA class II (Dr^+)					
CD3	NE	10	NE	31	≤ 15
CD4	NE	8	NE	26	≤ 15
CD8	NE	20	NE	51	≤ 15

NE indicates not evaluated; NR, not relevant.
*Blood investigation age.
†Patient 1 age-matched control values.
‡Patient 2 age-matched control values.

the age of 12 months. Corticosteroid treatment that consisted of high doses of intravenous methylprednisolone (1000 mg/1.73 m^2/d, injected for 3 days) followed by oral prednisone (1.5 mg/kg) for 2 months had no apparent clinical and radiologic benefits. Similarly, CSF investigations remained identical (Table 1).

Patient 2 was the second child of consanguineous parents from the same area of Algeria as family 1. The surnames of patients 1 and 2 were similar and further genetic analyses suggested that both families might be distantly related. Another sibling was healthy. Two maternal uncles died before 3 months of age in Algeria of unknown causes. Two paternal uncles also died in Algeria before the age of 2 years from "meningitis," although no further information was available. Birth weight and length were unknown. Neurologic symptoms were first retrospectively noted at the age of 6 months: poor head control and abnormal postural tone for age. The patient was admitted to an Algerian hospital for 2 episodes of "aseptic meningitis" at the ages of 7 and 12 months and because of seizures at the age of 24 months. Fever as well as CSF investigations were not documented at that time. He was first admitted to a French hospital 6 months later because of tetraparesis, cognitive impairment (developmental age, 15 months), and seizures. Hepatosplenomegaly was not detected. At that time, routine blood investigations were nearly normal except for hyperlymphocytosis (Table 1). To rule out metabolic diseases, we tested repetitively lactate level, acyl carnitine level, amino acid in plasma, and organic acids in urine and the results were normal. No evidence of low blood sugar was found. Finally, the mitochondrial respiratory chain was studied on mitochondria from lymphocytes, fibroblasts, and liver tissue by polarographic and spectrophometric assays and the results were normal. Brain MRI was performed. Large areas of white matter in the periventricular, deep supratentorial, and cerebellar areas were hyperintense in T2-weighted and FLAIR images and hypointense in T1-weighted images. Contrast enhancement was observed after gadolinium injection. There was also evidence of lesions in the corpus callosum (data not shown).

Three months later (33 months of age), patient 2 was admitted to our hospital with fever, weight loss, and anorexia. Clinical examination revealed massive hepatosplenomegaly. The results of laboratory investigations are shown in Table 1. Severe pancytopenia and a high percentage of HLA DR(+) CD4 and CD8 lymphocytes were observed. In addition, hypertriglyceridemia, hyponatremia, and lymphocytic meningitis were found. Transaminase, fibrinogen, and ferritin levels remained normal. Hemophagocytosis was observed on a bone marrow aspirate. Infection by herpes simplex viruses (HSVA-C), human herpes virus 6 (HHV6), cytomegalovirus (CMV), human immunodeficiency virus (HIV), adenovirus, bacteria, and fungi were excluded. Low copy number of EBV (0.8 log) was detected by PCR in the blood. CSF cultures were negative for bacteria and fungi. A normal level of interferon α (IFN-α; < 2 IU) was detected in the CSF, making viral infection highly unlikely. CSF lactate level was elevated. Treatment consisted of steroids and cyclosporine A (CsA). In 6 days, the hepatosplenomegaly, fever, and biomarkers of disease activity completely regressed, but on the seventh day, an acute neurologic deterioration occurred with coma and choreoathetoid movements. An MRI was performed, showing an extension of the lesions (Figure 1C).

Due to the patient's neurologic status, bone marrow transplantation was not considered. Steroids (2 mg/kg/d) and CsA were administered since the age of 2 years but remained ineffective. At 43 months of age, the patient was hospitalized for fever and

massive hepatosplenomagaly associated with biomarkers of disease activity and acute cholestatic hepatitis leading to death at the age of 44 months.

Detection of missense mutation in the perforin gene in both patients

Given the likelihood that both patients had FHL, we sought the molecular basis. Analysis of polymorphic markers showed a homozygous haplotype in both patients for the markers spanning the perforin locus (Figure 2A). Interestingly, both patients had inherited the same marker alleles. Direct sequencing identified an identical homozygous missense mutation within exon 3 of the gene in both patients. This mutation was a C > T transition at nucleotide position 1376, which leads to a proline to leucine substitution at position 459 of the protein. This mutation was also identified on one allele of the perforin gene in the parents but not in 132 control chromosomes, half of them being from the same geographic origin.

The 1376C>T mutation is located in the C2 phospholipid-binding domain of the protein

The C-terminal portion of perforin contains a C2 domain ending at the predicted site of cleavage, with calcium-dependent phospholipid-binding activity.[12] Based on its sequence, this C2 domain is predicted to be an 8-stranded β-sandwich, with a type II topology similar to that encountered in cytosolic phospholipase A2 (cPLA2) and phospholipase C δ (PLCδ).[12,16,17] The perforin C2 domain was modeled by using the proposed structure of cPLA2 as a template based on the alignment shown in Figure 3. The calcium-binding region, which is formed by 3 loops at the end of the β-sandwich, appeared to be conserved in perforin consistent with the findings of Uellner et al.[12] It contains residues required for calcium binding (Figure 3 arrow). The position affected by the identified mutation (P459) is highly conserved in all C2 domains. This position is located at the N-terminus of strand β4, at the end of loop 2 (Figure 3 *). It is preceded by a highly conserved asparagine, the Oδ1 atom,

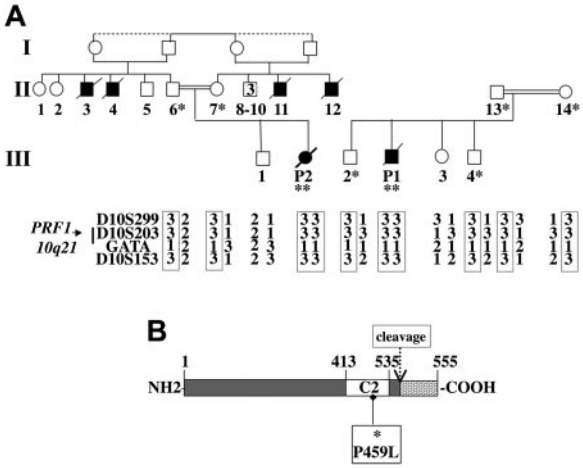

Figure 2. Family pedigrees, haplotype analysis of polymorphic markers spanning the perforin locus on chromosome 10q21, and mutation detection in the perforin gene. (A) Affected patients are homozygous at the perforin locus for all the markers tested. The same alleles of the markers spanning the perforin locus were inherited by patients 1 and 2, who belong to 2 different families. The same mutation was identified as homozygous (**) in the patients and heterozygous (*) in their parents and some of their siblings. (B) Schematic representation of the perforin protein. The open box represents the calcium-binding domain (C2) and the dashed box represents the C-terminal part of the protein that is cleaved during protein maturation. The missense mutation identified in the patients' perforin C2 domain is shown.

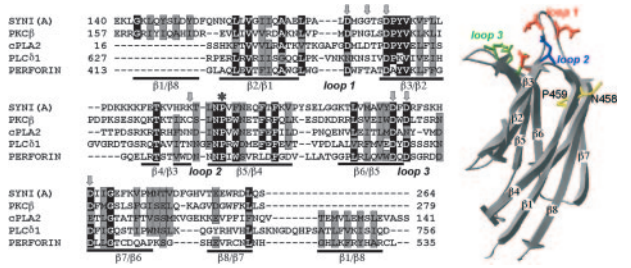

Figure 3. Structure of the perforin C2 domain. (Left) Alignment of the C2 domain of human perforin with C2 domains of known 3-dimensional structure (SYNI(A): first domain of synaptotagmin I, Protein Data Bank (pdb) identifier 1RSY; PKCβ: protein kinase C β, pdb identifier 1A25; cPLA2: cytoplasmic phospholipase A_2, pdb identifier 1rlw; PLCδ1: phosphoinositide-specific phospholipase C δ1, pdb identifier 1DJX). Identical amino acids are highlighted in black and similar amino acids are highlighted in gray. Mean positions of β-strands are indicated below the alignment, with labeling corresponding to the type I and type II topology. Amino acids that might be involved in calcium-binding sites are indicated by arrows (loop 1: D430, T433 [aligned with cPLA2 D40], D436 [the whole conformation of perforin loop 1 otherwise resembling more closely that of the loop 1 of synaptotagmin 1 C2A]; loop 2: D455 [aligned with cPLA2 N65]; loop 3: D484, D486, D492), whereas the position of the proline that is substituted by a leucine is shown by an asterisk. (Right) Model of the 3-dimensional structure of human perforin based on the proposed structure of cPLA2. Amino acids that might be involved in calcium binding are indicated, as are N458 and P459. Strands are labeled according to the type II topology, as predicted for human perforin.

which forms a hydrogen bond with the main chain N atom from a residue at the end of strand β1, just before loop 1. Replacement of proline by leucine is therefore expected to have a dramatic effect on the conformation of loop 2 and, more globally, on the conformation of the calcium-binding loops. Consequently, calcium binding might be severely impaired, although the chemical nature of residues directly involved in this binding is not affected.

The mutated perforin can mature and be expressed in cytotoxic granules but its function is impaired

Perforin is synthesized as a 70-kDa inactive glycosylated precursor, which is subsequently cleaved at the C-terminus to yield an active, mature form.[12] To determine whether the identified mutation impairs perforin cleavage, we assessed the perforin maturation in lymphocytes from patient 2. The 2d4-perforin monoclonal antibody, which recognizes both the mature and precursor forms of perforin,[12] detected the mature form in lymphocytes from patient 2 and from control subjects (Figure 4). Thus, this mutation does not impair perforin maturation. Flow cytometry analysis using the antiperforin dG9 antibody, which recognizes the native form of perforin only, detected a normal level of perforin in $CD8^+$ $TCR\alpha\beta^+$ cells from both patients, in contrast to cells from other FHL patients with a perforin mutation (as shown for P0 in Figure 4).[9,18] The perforin concentration was, however, slightly lower in NK ($TCR\alpha\beta^-$ $CD56^+$) cells from patients than in control NK cells (Figure 4). As perforin is a key effector of the cytotoxic activity of T and NK cells, we evaluated the cytotoxic activity of patients' lymphocytes. The cytotoxic activity of cells from both patients was strongly decreased similarly to perforin-deficient T cells (Figure 4). This defect in cytotoxic activity is not caused by impairment of the exocytosis of cytotoxic granules, as a similar quantity of granzyme A (BLT esterase) was released by activated lymphocytes from patients and controls (Figure 4). Thus, although the mutation identified in the perforin gene does not significantly affect perforin maturation and expression, it dramatically impairs perforin function, potentially by affecting the ability of the protein to bind calcium and thus target membrane phospholipids.

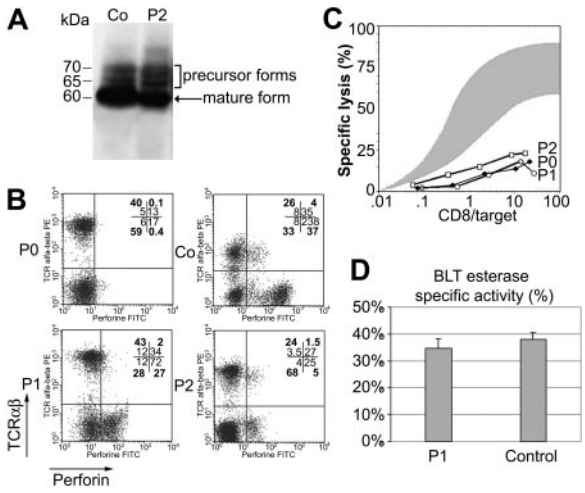

Figure 4. Perforin maturation, expression, cytotoxicity, and granule exocytosis assays using PBMCs from patients and controls. (A) Lysates were prepared from PHA blast lymphocytes from patient 2 (P2) and control subject (Co). Perforin was detected by immunoblotting with 2d4-perforin antibody under nonreducing conditions. One band corresponding to the mature form of perforin is seen in both subjects. (B) Perforin expression in the PBMCs of patients 1 (P1) and 2 (P2) compared with control PBMCs (Co) and PBMCs from a patient with a nonsense mutation in the perforin gene (P0); percent of gated cells in heavy type and MFI in normal type are indicated in each quadrant. (C) Cytotoxic activity of T lymphocytes from the 3 patients with a perforin defect (P1, P2, and P0) is defective compared with that of T cells from 20 age-matched controls (shaded area). The effector-to–target cell ratio (x-axis) reflects the ratio of $CD8^+$ T cells to target cells. Results are expressed as percentage of specific lysis (y-axis) as measured by ^{51}Cr release. (D) Secretion of granzyme A into the cell culture supernatant of CD3-activated $CD8^+$ T cells from P1 and Co was measured to quantify granule exocytosis. Cell supernatants were assayed by enzyme-linked immunosorbent assay (ELISA) for serine esterase. Data are expressed as the mean percentage ± SD specific release (test/total release) for triplicate samples.

Discussion

These 2 cases illustrate that the initial signs of FHL can present as a chronic encephalitis of subacute onset, which can precede systemic manifestations by several months or even years. Although primarily CNS findings have already been reported in FHL,[6,7,19] or in EBV-induced hemophagocytic syndrome,[20] the cases described here are the first ones molecularly characterized with such early onset of the neurologic symptoms and long delay between the onset of the neurologic symptoms and first clinical signs of systemic illness (ie, 27 months in patient 2). Of note, limited focal necrosis and parenchymal volume loss were observed in these cases compared with classical perforin-deficient FHL patients with neurologic involvement.[4,9] Both patients had an elevated CNS lactate concentration, which could have led to an erroneous diagnosis of metabolic disease at that age.

In these 2 families, FHL was caused by the same homozygous missense mutation in the perforin gene. This mutation affects neither perforin maturation by proteolytic processing nor its expression, although analysis of NK cells showed slightly less perforin in patients than in controls. The lytic granule content of lymphocytes was found to be released normally, but the perforin function of patients' lymphocytes was profoundly impaired. The fact that the mutation in the C2 domain of perforin affects a conserved structural residue of loop 2 of the calcium-binding site strongly suggests that the ability of perforin to bind calcium is impaired. This function of the C2 domain is expected to mediate binding of the protein to the phospholipid bilayer of the cytoplasmic membrane of the target cell.[12] Our findings thus strongly suggest that a calcium-binding step conferring activity to perforin is defective in patients with this condition.

The geographic origin of the patients and the results of our genetic analysis imply that both patients might be related and thus inherited the mutation from a common ancestor. Thus, the identical and atypical phenotype observed in both patients may be directly linked to this unique missense mutation in the perforin gene. It is indeed remarkable that most patients with classical systemic FHL carry either nonsense or missense mutations leading to the absence of perforin in their cytotoxic cells. These findings suggest that although the abnormal perforin was not functional in vitro, it could still have some residual function in vivo leading to a slightly attenuated phenotype. Alternatively, infection with an unidentified triggering microorganism might have primarily infected the CNS. Given their common origins, we cannot exclude the possibility that these patients had a common additional cosegregating genetic trait associated with or modifying the FHL phenotype. Further analyses of additional cases are required to evaluate the relationship between perforin gene mutation (allowing potential residual expression) and the clinical presentation of FHL. It will also be interesting to determine whether other patients with a similar clinical presentation carry perforin mutations and, if so, how these mutations affected gene expression.

These 2 cases show that some patients who do not fit the diagnostic guidelines for FHL during the initial stages of the disease[8] may be misdiagnosed when CNS involvement is predominant (and precedes systemic symptoms by some time). In addition, FHL should be considered in the differential diagnosis of acute necrotic encephalitis of unknown origin, especially in the absence of identified pathogens. Finding of mononuclear CSF pleocytosis and low natural killer cell or lymphocyte cytotoxic activity can support the diagnosis.

Acknowledgment

We thank Gillian M. Griffiths (Sir William Dunn School of Medicine, Oxford, United Kingdom) for the kind gift of perforin antibody 2d4-perf.

References

1. Stepp S, Dufourcq-Lagelouse R, Le Deist F, et al. Perforin gene defects in familial hemophagocytic lymphohistiocytosis. Science. 1999;286:1957-1959.
2. Feldmann J, Callebaut I, Raposo G, et al. Munc13–4 is essential for cytolytic granules fusion and is mutated in a form of familial hemophagocytic lymphohistiocytosis (FHL3). Cell. 2003;115:461-473.
3. Henter JI, Arico M, Elinder G, Imashuku S, Janka G. Familial hemophagocytic lymphohistiocytosis: primary hemophagocytic lymphohistiocytosis. Hematol Oncol Clin North Am. 1998;12:417-433.
4. Haddad E, Sulis ML, Jabado N, Blanche S, Fischer A, Tardieu M. Frequency and severity of central nervous system lesions in hemophagocytic lymphohistiocytosis. Blood. 1997;89:794-800.
5. Henter JI, Nennesmo I. Neuropathologic findings and neurologic symptoms in twenty-three children with hemophagocytic lymphohistiocytosis. J Pediatr. 1997;130:358-365.
6. Kieslich M, Vecchi M, Driever PH, Laverda AM, Schwabe D, Jacobi G. Acute encephalopathy as a primary manifestation of haemophagocytic lymphohistiocytosis. Dev Med Child Neurol. 2001;43:555-558.

7. Henter JI, Elinder G. Cerebromeningeal haemophagocytic lymphohistiocytosis. Lancet. 1992; 339:104-107.
8. Henter JI, Elinder G, Ost A. Diagnostic guidelines for hemophagocytic lymphohistiocytosis: the FHL Study Group of the Histiocyte Society. Semin Oncol. 1991;18:29-33.
9. Feldmann J, Le Deist F, Ouachee-Chardin M, et al. Functional consequences of perforin gene mutations in 22 patients with familial haemophagocytic lymphohistiocytosis. Br J Haematol. 2002; 117:965-972.
10. Dufourcq-Lagelouse R, Jabado N, Le Deist F, et al. Linkage of familial hemophagocytic lymphohistiocytosis to 10q21–22 and evidence for heterogeneity. Am J Hum Genet. 1999;64:172-179.
11. Callebaut I, Labesse G, Durand P, et al. Deciphering protein sequence information through hydrophobic cluster analysis (HCA): current status and perspectives. Cell Mol Life Sci. 1997;53: 621-645.
12. Uellner R, Zvelebil MJ, Hopkins J, et al. Perforin is activated by a proteolytic cleavage during biosynthesis which reveals a phospholipid-binding C2 domain. EMBO J. 1997;16:7287-7296.
13. Guex N, Peitsch MC. SWISS-MODEL and the Swiss-PdbViewer: an environment for comparative protein modeling. Electrophoresis. 1997;18: 2714-2723.
14. Sali A, Potterton L, Yuan F, van Vlijmen H, Karplus M. Evaluation of comparative protein modeling by MODELLER. Proteins. 1995;23:318-326.
15. Ménasché G, Pastural E, Feldmann J, et al. Mutations in RAB27A cause Griscelli syndrome associated with hemophagocytic syndrome. Nat Genet. 2000;25:173-176.
16. Rizo J, Sudhof TC. C2-domains, structure and function of a universal Ca2+-binding domain. J Biol Chem. 1998;273:15879-15882.
17. Nalefski EA, Falke JJ. The C2 domain calcium-binding motif: structural and functional diversity. Protein Sci. 1996;5:2375-2390.
18. Arico M, Allen M, Brusa S, et al. Haemophagocytic lymphohistiocytosis: proposal of a diagnostic algorithm based on perforin expression. Br J Haematol. 2002;119:180-188.
19. Rostasy K, Kolb R, Pohl D, et al. CNS disease as the main manifestation of hemophagocytic lymphohistiocytosis in two children. Neuropediatrics. 2004;35:45-49.
20. Imashuku S. Clinical features and treatment strategies of Epstein-Barr virus-associated hemophagocytic lymphohistiocytosis. Crit Rev Oncol Hematol. 2002;44:259-272.